International Journal of Electrical, Electronic and Communication Sciences
ISSN: 2517-9438
Vol:6, No:12, 2012

Thermal Analysis of the Fuse with Unequal Fuse Links Using Finite Element Method

Adrian T. Pleşca

***Abstract*—**In this paper a three dimensional thermal model of high breaking capacity fuse with unequal fuse links is proposed for both steady-state or transient conditions. The influence of ambient temperature and electric current on the temperature distribution inside the fuse, has been investigated. A thermal analysis of the unbalanced distribution of the electric current through the fuse elements and their influence on fuse link temperature rise, has been performed. To validate the three dimensional thermal model, some experimental tests have been done. There is a good correlation between experimental and simulation results.

***Keywords*—**Electric fuse, fuse links, temperature distribution, thermal analysis.

I. Introduction

A fuse is generally accepted to be the simplest form of protection device used to avoid damage to an electrical system by excess currents. This view stems from the simple construction of the wire type fuse and often leads to the assumption that the operation of a fuse is also simple. In general terms, the fuse is an electrical conductor, which melts when subjected to excessive current and due to disintegration subsequently interrupts current flow. The fuse is then irreparably damaged and can be viewed as being forfeited in the process of protecting the electrical system. Besides interrupting fault currents a fuse should conduct current for all conditions except those classed as faults. Furthermore after operation a fuse should present a high resistance to current flow. These attributes are fundamental to the role of the fuse but are commonly overlooked by all but the specialist. More complex attributes of fuse operation, of interest to fuse designers and specialist users, are the requirements to avert potentially circuit-damaging disturbances generated during disintegration and furthermore to quickly force current interruption. These and other attributes are important in the role of semiconductor and high breaking capacity current limiting fuses.

All modern high breaking capacity fuses contain elements, usually with restrictions, of small cross-sectional areas connected between relatively massive end connections which act as heat sinks. To obtain rapid operation this principle is employed to a high degree. Due to non-linear geometry of the fuse links and because some physical parameters such as electrical resistivity, thermal conductivity and specific heat have important variations with the temperature [1], it is not possible to carry out the thermal study using standard analytical equations and it is necessary to apply numerical methods in order to get a valid thermal model of fuse behaviour.

Approaches to simulate the fuse thermal processes have already been made in earlier work. In [2] the temperature distribution, and the thermal and electrical resistances of basic elements of the fuses are described by exact or semi-empirical analytical equations, and combined with iterative solution procedures. In [3],[4] the fuse link is represented by an equivalent R-C network. Other simulations discretize the fuse link including its conductor according to finite element, in [5]-[8], or finite difference schemes, like in [9]. Numerical methods for studying the prearcing times of high breaking capacity fuses and including solid - liquid - vapour phase changes of the fuse element, are reported in [10]-[12]. Thermal behaviour of fast fuses used to protect power semiconductors such as power diodes and thyristors, using 3-D Finite Element Method (FEM), is presented in [13]. Because of the typical geometry of fuses a three-dimensional discretization is generally necessary, at least for the heat diffusion problem. In [14], [15] a commercial FEM package has been used to model heating of relatively simple fuse geometries without notches and with one single notch, respectively. Other FEM work has been reported in [16]-[19]. In [20] a thermal model of the fuse including M-Effect using the finite volume method, has been developed. Also, a thermal analysis of a medium voltage fuse by means of the finite element method is presented in [21].

This study attempts to achieve and validate a three dimensional thermal model of high breaking capacity fuses with unequal fuse links.

II. Thermal Model

The aim of this study is to develop a three dimensional model of a high breaking capacity fuse with unequal fuse elements. The basic equation of heat transfer has the following expression for each volume element dV:

$$Q_c = Q_t - Q_r + Q_a \tag{1}$$

The left term of the equation is the heating power from the current flow, Q_c. It is in balance with the heat stored by temporal change of temperature Q_t, the power removed from the element by thermal conduction Q_r, and the thermal power dissipated to the surrounding area by the surface convection,

A. T. Pleşca is with the Gheorghe Asachi Technical University of Iasi, Iasi, IS 700050 Romania (phone: 40-232-278683; fax: 40-232-237627; e-mail: aplesca@ee.tuiasi.ro).

Q_a. For the above thermal power quantities, the following equations can be written:

$$Q_c = \iiint \rho j^2 dV; \quad Q_t = \iiint \gamma c \frac{\partial \theta}{\partial t} dV;$$
$$Q_r = \iiint div(\lambda \cdot grad\theta) dV; \quad (2)$$
$$Q_a = \iiint k \frac{l}{S_f}(\theta - \theta_a) dV$$

where:
- ρ means the electrical resistivity;
- j – current density;
- γ – material density;
- c – specific heat;
- λ – thermal conductivity;
- θ – temperature;
- θ_a – ambient temperature;
- k - convection coefficient;
- l – perimeter length of the fuse link cross-section;
- S_f – cross-section of the fuse link.

Therefore,

$$\iiint \rho j^2 dV = \iiint \gamma c \frac{\partial \theta}{\partial t} dV - \iiint div(\lambda \cdot grad\theta) dV + \quad (3)$$
$$+ \iiint k \frac{l}{S_f}(\theta - \theta_a) dV$$

Because the fuse link has a variable cross-section and the physical parameters, especially the electrical resistivity, vary with the temperature, the above equation is a non-linear type with variable coefficients and it demands a numerical procedure to evaluate the temperature distribution. It is desirable to restate the problem by considering various forms of discretization. The discretised form of the problem only requires the solution to be satisfied at a finite number of points in the region; and in the remainder of the region, appropriate interpolations may be used. Thus, this case is reduced to an algebraic form involving only the basic arithmetic operations, which could in turn be solved by numerical methods. These methods have become very accurate and reliable for solving initial and boundary value problems. The basic idea of the finite element method is to discretise the domain V, into several subdomains, or finite elements. These elements can be irregular and possess different properties so that they form a basis to discretise complex structures, or structures with mixed material properties. Using Galerkin's method and including convection boundary condition, the discretized equations for the heat transfer are as follows:

$$\int_V \rho j^2 N_i dV = \int_V \gamma c \frac{\partial \theta}{\partial t} N_i dV + \int_V \left[\frac{\partial N_i}{\partial x} \quad \frac{\partial N_i}{\partial y} \quad \frac{\partial N_i}{\partial z}\right] \lambda [B]\{\theta\} dV +$$
$$+ \int_S k(\theta - \theta_a) N_i dS \quad (4)$$

where [N] is the matrix of shape functions and [B] is the matrix for temperature gradients interpolation. Shape functions N_i are used for interpolation of temperature and temperature gradients inside a finite element:

$$\theta = [N]\{\theta\}, \quad [N] = [N_1 \ N_2 \ N_3 ...], \quad \{\theta\} = \{\theta_1 \ \theta_2 \ \theta_3 ...\}$$
$$\begin{Bmatrix} \frac{\partial \theta}{\partial x} \\ \frac{\partial \theta}{\partial y} \\ \frac{\partial \theta}{\partial z} \end{Bmatrix} = \begin{bmatrix} \frac{\partial N_1}{\partial x} & \frac{\partial N_2}{\partial x} & \frac{\partial N_3}{\partial x} ... \\ \frac{\partial N_1}{\partial y} & \frac{\partial N_2}{\partial y} & \frac{\partial N_3}{\partial y} ... \\ \frac{\partial N_1}{\partial z} & \frac{\partial N_2}{\partial z} & \frac{\partial N_3}{\partial z} ... \end{bmatrix} \{\theta\} = [B]\{\theta\} \quad (5)$$

The finite element equations corresponding to the heat transfer have the following matrix form:

$$[A]\{\dot{\theta}\} + ([L_c] + [L_k])\{\theta\} = \{R_Q\} + \{R_k\} \quad (6)$$

$$[A] = \int_V [N]^T \gamma c [N] dV; \quad [L_c] = \int_V [B]^T \lambda [B] dV;$$
$$[L_k] = \int_S [N]^T k [N] dS \quad (7)$$

$$[R_Q] = \int_V \rho j^2 [N]^T dV; \quad [R_k] = \int_S k\theta_a [N]^T dS \quad (8)$$

A three dimensional model for a high breaking capacity fuse has been developed using specific software like Pro-ENGINEER, which is an integrated thermal design tool for all type of accurate thermal analysis on devices. The fuse was a gG type, size 2, with rated current by 160A, rated voltage about 550V, rated power losses of 12.8W and rated breaking capacity of 120kA. The 3D model had taken into consideration all the component parts of a high breaking capacity fuse: inner and outer cap, silica sand, ceramic body, alloy M-effect attached on both fuse links and knife contacts, as shown in Fig. 1. It was considered a simplified geometry for the screws.

III. Thermal Simulations

The technological and mounting processes (punching, spot welding) of the fuse links inside the fuse lead to different dimensions (length, thickness) for the fuse elements. This means different electrical resistance of the fuse links which leads to an unequal current distribution through the fuse links when the fuse includes more fuse elements mounted in parallel. Hence, from the total current I, which flows through the fuse, the current I_1 will pass through the fuse link F1 and the current I_2 will flow through the other fuse link F2. It will consider an asymmetry coefficient a, $1 \leq a \leq 2$, which describes the unbalanced current distribution through the fuse links. Supposing $I_1 = aI_2$ and $I_1 + I_2 = I$, results:

$$I_1 = \frac{a}{a+1} I; \quad I_2 = \frac{1}{a+1} I \quad (9)$$

The voltage drop along the parallel fuse links is,

$$U = R_1 I_1 = R_2 I_2 \quad (10)$$

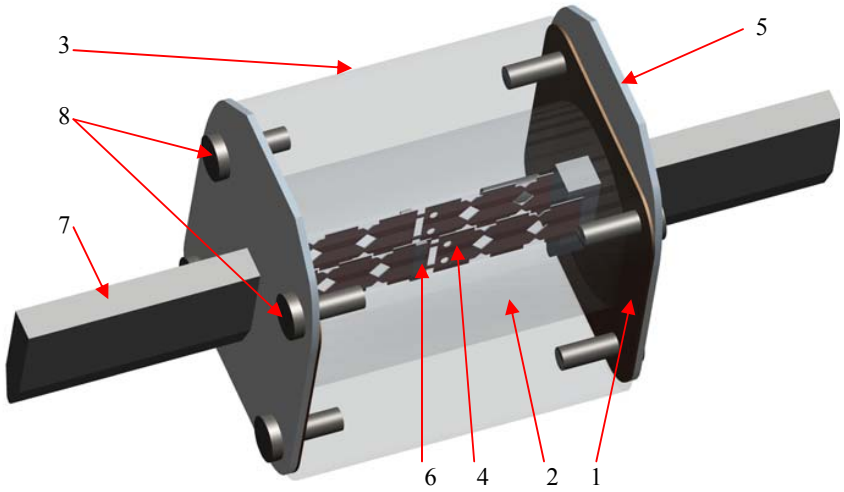

Fig. 1 Thermal model of the high breaking capacity fuse (1 – inner cap; 2 – silica sand; 3 – ceramic body; 4 – fuse link; 5 – outer cap; 6 – alloy M-effect; 7 – knife contact; 8 – screws)

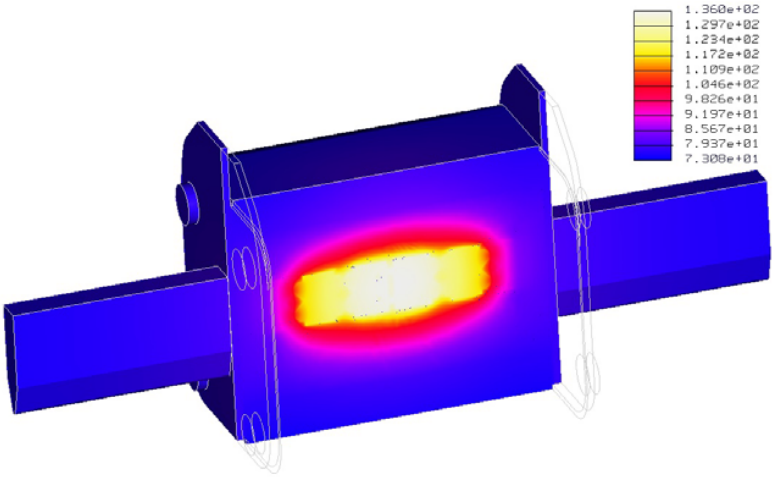

Fig. 2 Temperature distribution through the most thermally loaded fuse link, at current value of 200A and asymmetry coefficient equal with 2

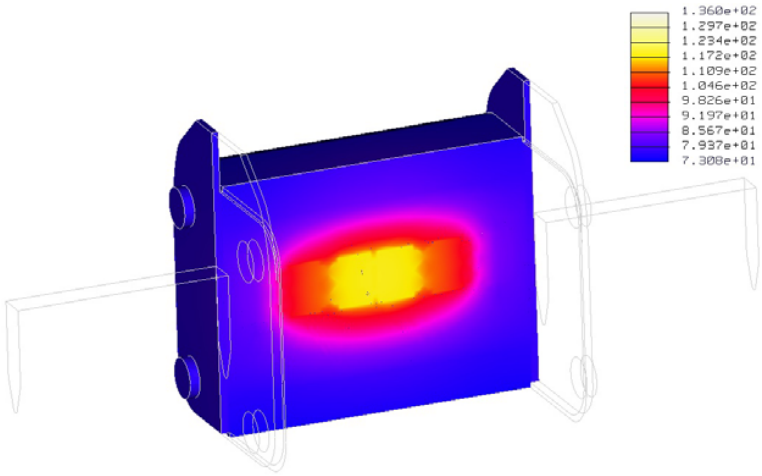

Fig. 3 Temperature distribution through the least thermally loaded fuse link, at current value of 200A and asymmetry coefficient equal with 2

and taking into account the hypothesis $I_1 = aI_2$, results,

$$R_1 = \frac{R_2}{a} \tag{11}$$

The power losses for both fuse links have the well known expressions:

$$P_1 = R_1 I_1^2; \quad P_2 = R_2 I_2^2 \text{ and } P_1 + P_2 = P \tag{12}$$

Including (9) and (11) in (12), it obtains the following expressions for the power losses,

$$P_1 = \frac{a}{a+1} P; \quad P_2 = \frac{1}{a+1} P \tag{13}$$

When the asymmetry coefficient a = 1, results equal power losses for both fuse links, $P_1 = P_2 = P/2 = 6.4$W.

The 3D finite elements Pro-MECHANICA software has been used for all thermal simulations. The material properties of every component part of the fuse are described in the Table 1, according to Fig. 1. The heat load has been applied on both fuse link elements depending on the asymmetry coefficient which has been considered. There is a uniform spatial distribution on these elements. The mesh of this 3D fuse thermal model has been done using tetrahedron solids element types with the following allowable angle limits (degrees): maximum edge: 175; minimum edge: 5; maximum face: 175; minimum face: 5. The maximum aspect ratio was 30 and the maximum edge turn (degrees): 95. The single pass adaptive convergence method to solve the thermal steady-state simulation has been used.

TABLE I
MATERIAL DATA AND COEFFICIENTS AT 20°C ACCORDING WITH THE COMPONENT PARTS FROM FIG. 1

Material	Parameter		
	γ (kg/m^3)	c (J/kgºC)	λ (W/mºC)
Ceramic/ Steatite C221 (3)	2700	900	2.6
Copper (4)	8900	385	385
Iron FE40 (8)	7190	420.27	52.028
Brass (7)	8550	386	115
Aluminium (5)	2700	890	220
Alloy SnCu1 (6)	7310	217	67
Insulation material/ pressed carton (1)	1400	0.099	0.063
Silica sand (2)	830	1201	1

The analyzed fuse has the following overall dimensions: length of the ceramic body: 61mm, square cross-section: 50mm x 50mm, total length including the knife contacts: 150mm. The fuse link has a length of 55mm, width about 10mm and thickness of 0.2mm. The ambient temperature was about 25ºC. From experimental tests [22], it was computed k = 15.3W/m^{2}ºC on the ceramic body. For all metal component parts of the fuse, the convection coefficient was about 19.5W/m^{2}ºC. It was considered the convection condition like boundary condition for the outer boundaries such as outer caps, knife contacts, screws, ceramic body and it has been applied on surfaces with an uniform spatial variation and a bulk temperature of 25ºC.

Further on, some steady state thermal simulations have been done. The temperature distribution inside the fuse through the most thermally loaded fuse link is shown in Fig. 2 and through the least thermally loaded fuse element is presented in Fig. 3. In Fig. 4 is shown the temperature distribution at a half cross-section through whole fuse. It is to observe the higher temperatures on the right side of the fuse cross-section which match to the most thermally loaded fuse link. In order to better outline the fuse links temperature distribution, in Fig. 5 only the fuse elements are depicted.

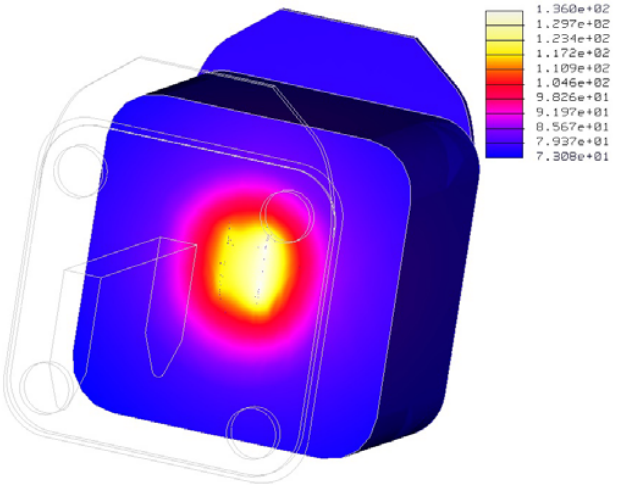

Fig. 4 Temperature distribution through the fuse at 50% cross-section for electric current value of 200A and asymmetry coefficient equal with 2

The fuse link lengthwise temperature distributions for different asymmetry coefficients and current values are presented in Fig. 6 and Fig. 7. Temperature distribution along the fuse links for different ambient temperatures is shown in Fig. 8. In all cases, a comparison between the most and the least thermally loaded fuse link, has been done.

In order to analyse the time evolution of the temperature rise for both fuse links, a series of transient thermal simulations have been done. The measure point was considered in the middle of the both fuse link elements, actually the hot spot temperature. The time temperature evolution at rated current of 160A and different asymmetry coefficients is presented in Fig. 9. A comparison between time temperature evolutions at different current values and the asymmetry coefficient equal with 2, is shown in Fig. 10.

IV. DISCUSSION OF THE RESULTS

As it can be seen from Fig. 2, Fig. 3 and Fig. 5, the maximum temperature is obtained in the middle of the fuse link elements.

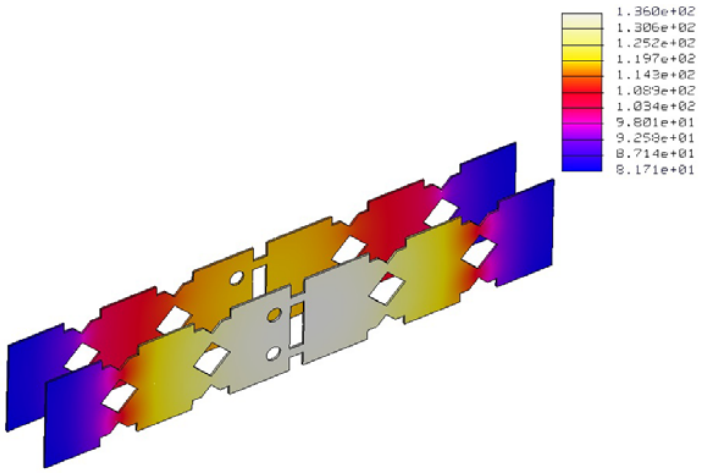

Fig. 5 Temperature distribution only for both fuses links at electric current value of 200A and asymmetry coefficient equal with 2

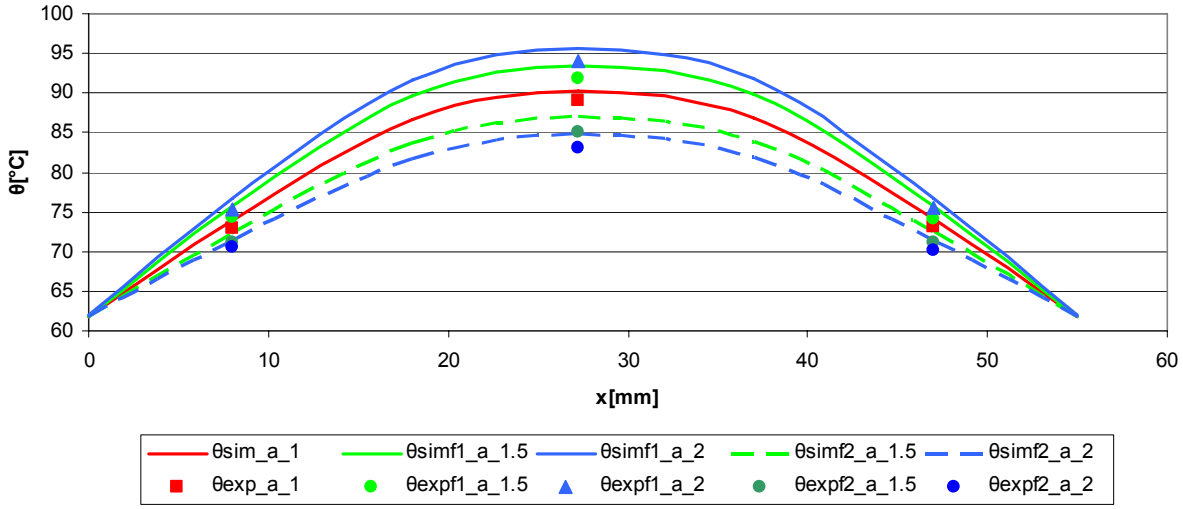

Fig. 6 Temperature distribution along the fuse links for current value of 160A and different asymmetry coefficient a =1; 1.5; 2. Comparison between simulation (θsim_a_1, θsimf1_a_1.5, θsimf1_a_2, θsimf2_a_1.5, θsimf2_a_2) and experimental values (θexp_a_1, θexpf1_a_1.5, θexpf1_a_2, θexpf2_a_1.5, θexpf2_a_2)

This is due to the notches made on the fuse links in order to clear the fault current as soon as possible and to interrupt the electric circuit without high over voltages. In Fig. 4 is shown the temperature distribution through the fuse at 50% cross-section with the aim to outline the difference between maximum temperatures of both fuse links. The thermal simulations have been performed considering an electric current of 200A, the asymmetry coefficient equal with 2, and the ambient temperature about 25°C. The maximum temperature for the most thermally loaded fuse link is 135.59°C and for the least thermally loaded fuse link is about 119.31°C.

The fuse link lengthwise temperature distribution at different values of asymmetry coefficient, in the case of total current through the fuse equal with the rated one, is shown in Fig. 6.

It can be noticed the increasing of the difference between maximum temperatures of the most thermally loaded fuse link (θsimf1_a_1.5, θsimf1_a_2) and the least thermally loaded fuse link (θsimf2_a_1.5, θsimf2_a_2). When the asymmetry coefficient is equal with 2, this difference is about 10.84°C. A comparison between fuse links lengthwise temperature distribution for current variation from 120 to 200A, with the asymmetry coefficient a = 2, is presented in Fig. 7. As expected, when the current increases, the difference between maximum temperatures of the fuse links increases too. Thus, at the current value of 200A, the maximum temperature of the most thermally loaded fuse link (θsimf1_200A) is 135.59°C and the maximum temperature of the least thermally loaded fuse link (θsimf2_200A) is 118.31°C.

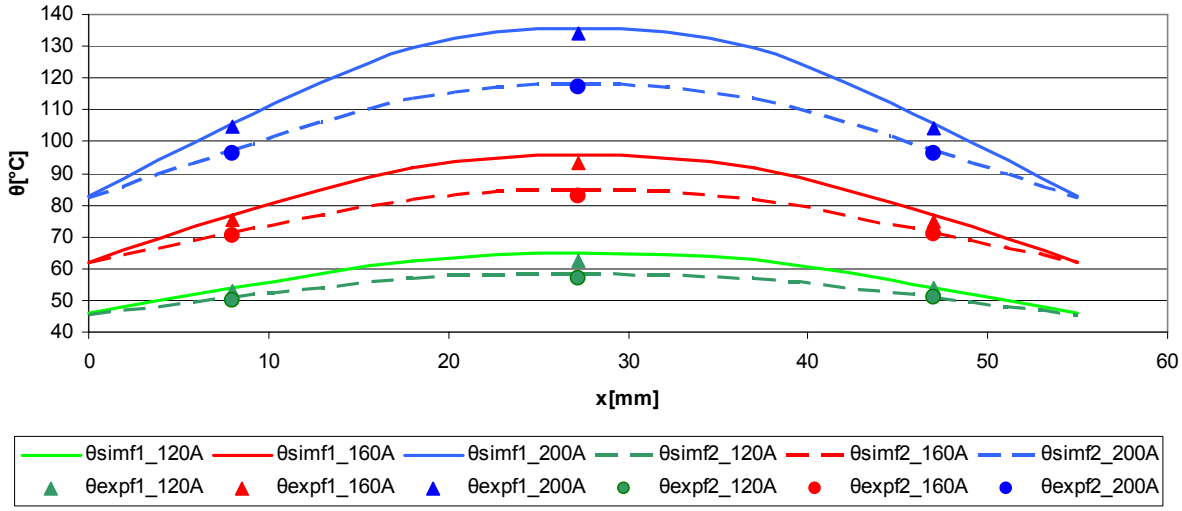

Fig. 7 Temperature distribution along the fuse links for current value of 120, 160 and 200A and asymmetry coefficient a = 2. Comparison between simulation (θsimf1_120A, θsimf1_160A, θsimf1_200A, θsimf2_120A, θsimf2_160A, θsimf2_200A) and experimental values (θexpf1_120A, θexpf1_160A, θexpf1_200A, θexpf2_120A, θexpf2_160A, θexpf2_200A)

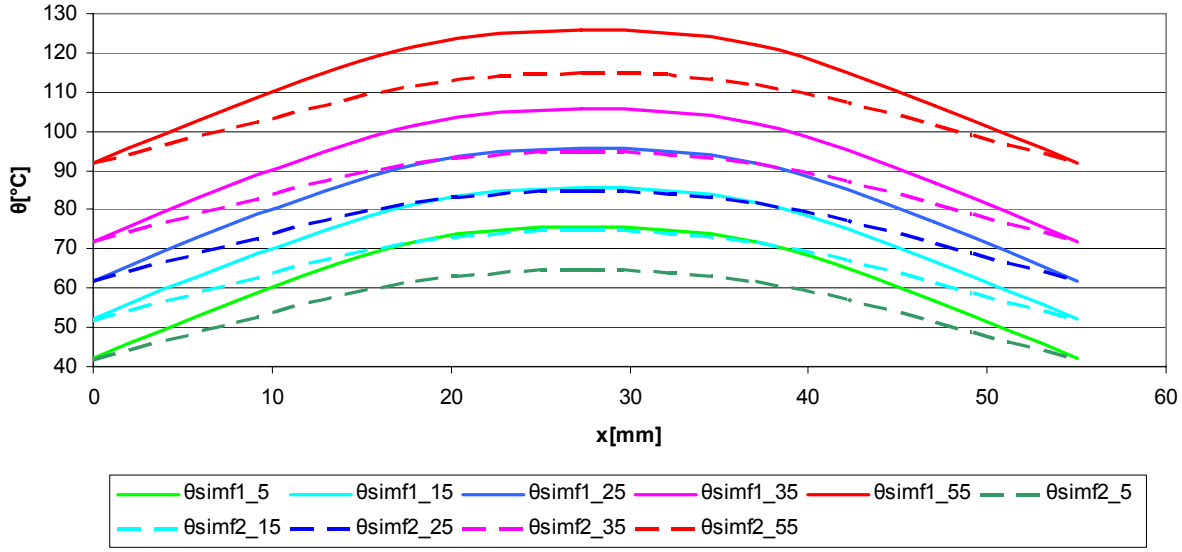

Fig. 8 Temperature distribution along the fuse links for ambient temperature of 5, 15, 25, 35 and 55°C. Comparison between simulation results of the most thermally loaded fuse link (θsimf1_5, θsimf1_15, θsimf1_25, θsimf1_35, θsimf1_55) and the least thermally loaded fuse link (θsimf2_5, θsimf2_15, θsimf2_25, θsimf2_35, θsimf2_55)

When the ambient temperature varies from 5 to 55°C (Fig. 8), the temperature distribution curves along the fuse links, translates on vertical direction, from the maximum temperature of 75.66 to 125.66°C in the case of the most thermally loaded fuse link, and from 64.82 to 114.82°C in the case of the least thermally loaded fuse link. The current through the fuse was at the value of 160A, the rated one.

The time evolutions of the maximum temperature of the fuse links when the asymmetry coefficient varies from 1 to 2 at the total current of 160A through the fuse, are depicted in Fig. 9.

It can be noticed that there was a relatively fast increase in the temperature and that after approximately 4000 seconds, the values are stabilized. A comparison between time evolutions of the maximum temperatures of both fuse links at different current values (from 160 to 200A) when the asymmetry coefficient was equal with 2, is presented in Fig. 10. In this case, the temperatures achieve the steady-state conditions after approximate 4500 seconds.

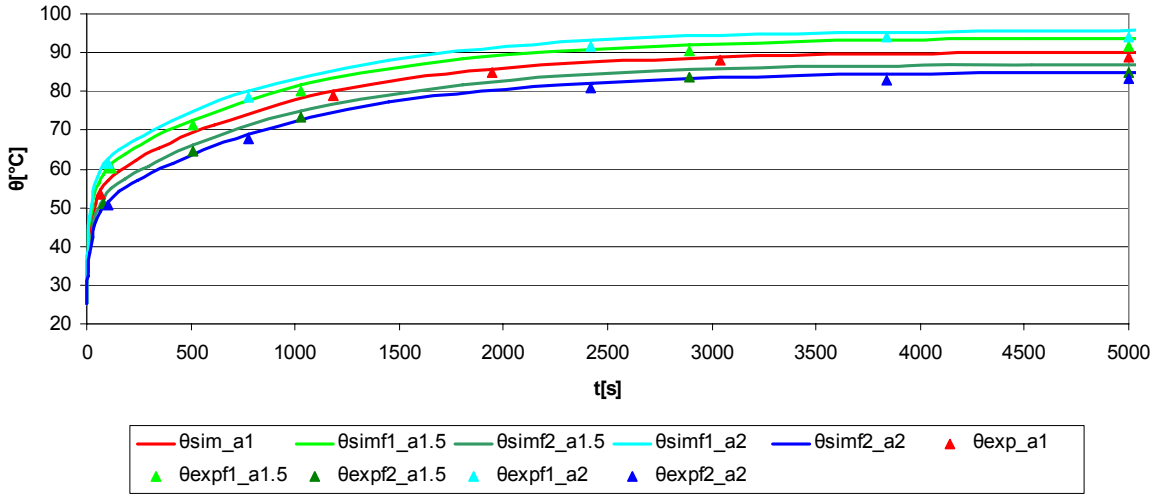

Fig. 9 Maximum fuse links temperature time evolution for current value of 160A and different asymmetry coefficient a =1; 1.5; 2. Comparison between simulation (θsim_a1, θsimf1_a1.5, θsimf1_a2, θsimf2_a1.5, θsimf2_a2) and experimental values (θexp_a1, θexpf1_a1.5, θexpf1_a2, θexpf2_a1.5, θexpf2_a2)

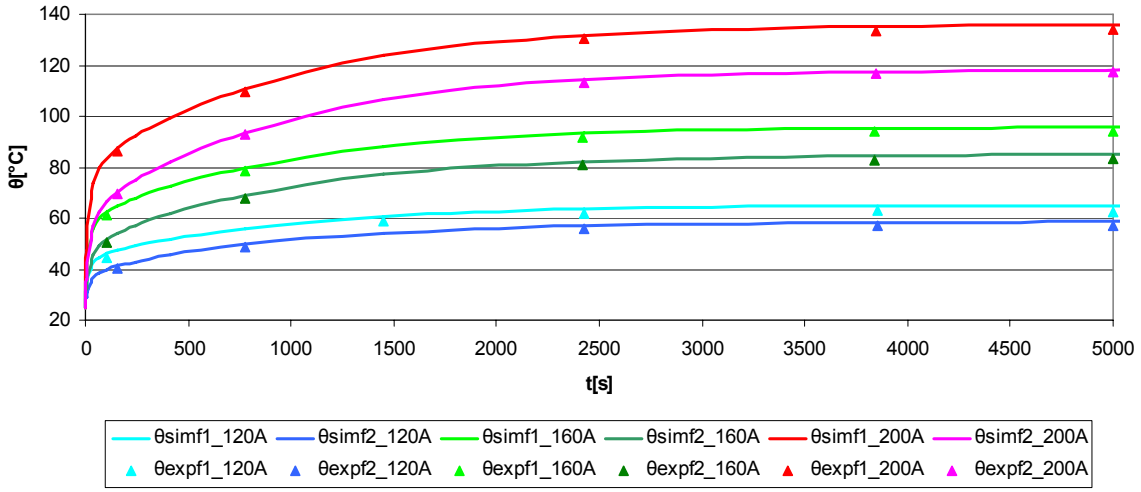

Fig. 10 Maximum fuse links temperature time evolution for current value of 120, 160 and 200A with the asymmetry coefficient a = 2. Comparison between simulation (θsimf1_120A, θsimf1_160A, θsimf1_200A, θsimf2_120A, θsimf2_160A, θsimf2_200A) and experimental values (θexpf1_120A, θexpf1_160A, θexpf1_200A, θexpf2_120A, θexpf2_160A, θexpf2_200A)

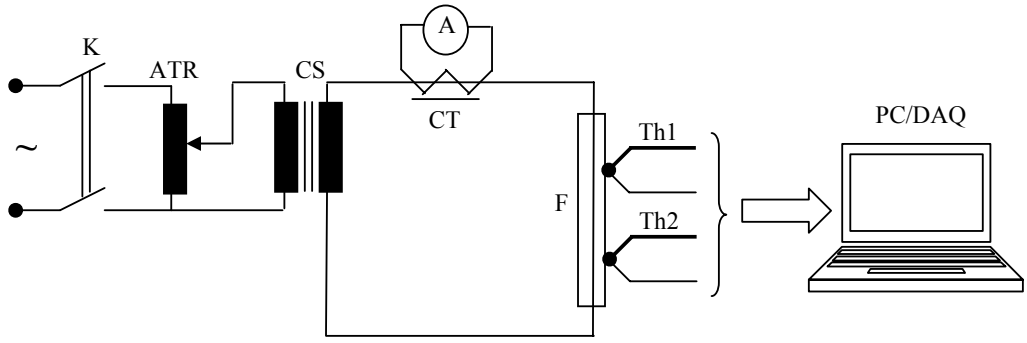

Fig. 11 Experimental main circuit

To validate the simulation results, some experimental tests have been made with the same conditions as in the case of thermal simulations. The electric circuit diagram used for experimental tests is shown in Fig. 11.

The main switch K, enables the supply with low-voltage for the auto-transformer ATR, which adjusts the input voltage for the current supply device CS. The high current from CS, flows through the high breaking capacity fuse F, and will warm it. The current value is measured by an ammeter A, through a current transformer CT. Using proper thermocouples Th1, Th2, type K, the temperatures in the middle and end terminals of both fuse links have been acquired. The measurement points are the same as during the thermal simulations. The small voltage signals provided by thermocouples have been amplified using a signal conditioning board type AT2F-16. The amplified signal was the input for a data acquisition board type PC-LPM-16 which can be programmed with LabVIEW software. The comparisons between simulation and experimental results are presented in Fig. 6, Fig. 7 and Fig. 9, Fig. 10. The experimental temperature values are smaller than the computation results. This is because during the experimental tests, the fuse was mounted on its fuse-carrier and there are conductors to connect the fuse with electric circuit. Because of their volume and thermal capacity, these entire components act like real heat sinks for the fuse links, resulting in an important heat dissipation rate. On the other hand, the differences between the temperature values resulting from experimental tests and those obtained during simulations are due to various factors: measurement errors, thermal model simplifications and mounting test conditions. Nevertheless, the maximum difference between the experimental and simulation results is less than 3ºC.

V. Conclusion

The obtained three dimensional thermal model allows analysis of the thermal behaviour of high breaking capacity fuses with unequal fuse links parallel mounted. The thermal model provides the fuse links lengthwise temperature distribution at different currents, ambient temperature values and asymmetry coefficient variation and could be used as a designing tool for the power systems protection, especially at low voltage power supply. Some experimental tests have been made in order to validate the proposed three dimensional thermal model. There is a good correlation between experimental and simulated results. Using the proposed thermal model, the fuse design process can be improved and there is the possibility of obtaining new solutions for a better correlation between fuses and protected devices.

Acknowledgment

This work was supported by CNCSIS – UEFISCDI, project number 515 PNII – CAPACITATI, 2011.

References

[1] A. Wright, and P. G. Newbery, *Electric Fuses.* London: IEE, 2004, ch.3

[2] R. Wilkins, "Steady-state current sharing in fuses with asymmetrical arrangements," in *Proc. of the 4th Int. Conf. on Electric Fuses and their Applications,* Nottingham, 1991, pp. 28-33.

[3] J. Gelet, D. Tournier, and M. Ruggiero, "Evaluation of thermal and electrical behaviour of fuses in case of paralleling and/or high frequencies," in *Proc. of the 6th Int. Conf. on Electric Fuses and their Applications,* Torino, 1999, pp. 49-53.

[4] G. Hoffmann, and U. Kaltenborn, "Thermal modelling of high voltage H.R.C. fuses and simulation of tripping characteristic," in *Proc. of the 7th Int. Conf. on Electric Fuses and their Applications*, Gdansk, 2003, pp. 174-180.

[5] H. Kürschner, A. Ehrhardt, and G. Nutsch, "Calculation of prearcing times using the Finite Element Method," in *Proc. of the 5th Int. Conf. on Electric Fuses and their Applications,* Ilmenau, 1995, pp. 156-161.

[6] L. Fernández, C. Cañas, J. Llobell, J. Curiel, J. Aspas, J. Ruz, and F. Cavallé, "A model for pre-arcing behaviour simulation of H.V. full-range fuse-links using the finite element method," in *Proc. of the 5th Int. Conf. on Electric Fuses and their Applications,* Ilmenau, 1995, pp. 162-168.

[7] M. Wilniewczyc, P.M. McEwan, and D. Crellin, "Finite-element analysis of thermally-induced film de-bonding in single and two-layer thick-film substrate fuses," in *Proc. of the 6th Int. Conf. on Electric Fuses and their Applications,* Torino, 1999, pp. 29-33.

[8] Z. Guobiao, H. Chenming, P. Y. Yu, S. Chiang, S. Eltoukhy, and E. Z. Hamdy, "An electro-thermal model for metal-oxide-metal antifuses," *IEEE Tran. On Electron Devices*, vol. 42, pp. 1548-1558, 1995.

[9] C. Garrido, and J. Cidrás, "Study of fuselinks with different t-I curves using a mathematical model," in *Proc. of the 6th Int. Conf. on Electric Fuses and their Applications,* Torino, 1999, pp. 21-24.

[10] D. Rochette, R. Touzani, and W. Bussière, "Numerical study of the short pre-arcing time in high breaking capacity fuses via an enthalpy formulation," *J. Phys. D: Appl. Phys.*, vol. 40, pp. 4544-451, 2007.

[11] S. Memiaghe, W. Bussière, and D. Rochette, "Numerical method for pre-arcing times : application in HBC fuses with heavy fault-currents," in *Proc. of the 8th Int. Conf. on Electric Fuses and their Applications*, Clermont-Ferrand, 2007, pp. 127-132.

[12] D. Rochette, W. Bussiere, R. Touzani, S. Memiaghe, G. Velleaud, and P. Andre, "Modelling of the pre-arcing period in HBC fuses including solid - liquid - vapour phase changes of the fuse element," in *Proc. of the 8th Int. Conf. on Electric Fuses and their Applications*, Clermont-Ferrand, 2007, pp. 87 – 93.

[13] Y. Kawase, T. Miyatake, and S. Ito, "Heat analysis of a fuse for semiconductor devices protection using 3-D finite element method," *IEEE Trans. on Magnetics*, vol. 36, pp. 1377 – 1380, 2000.

[14] D. A. Beaujean, P. G. Newbery, and M. G. Jayne, "Modelling fuse elements using a C.A.D. software package," in *Proc. of the 5th Int. Conf. on Electric Fuses and their Applications,* Ilmenau, 1995, pp. 133-142.

[15] A. Petit, G. St-Jean, and G. Fecteau, "Empirical model of a current-limiting fuse using EMTP," *IEEE Trans. On Power Delivery*, vol. 4, pp. 335-341, 1989.

[16] C. Cañas, L. Fernández, and R. González, "Minimum breaking current obtaining in fuses," in *Proc. of the 6th Int. Conf. on Electric Fuses and their Applications,* Torino, 1999, pp. 69-74.

[17] K. Jakubiuk, and W. Aftyka, "Heating of fuse-elements in transient and steady-state," in *Proc. of the 7th Int. Conf. on Electric Fuses and their Applications,* Gdansk, 2003, pp. 181-187.

[18] H.F. Farahani, M. Asadi, and A. Kazemi, "Analysis of thermal behavior of power system fuse using finite element method," in *Proc. of the 4th Int. Power Engineering and Optimization Conference*, 2010, pp. 189 – 195.

[19] A. Hamler, S. Gril, and J. P. Cukovic, "Thermal analysis and temperature calculation for the NV melting fuse," in *Proc. of the 9th Int. Conf. on Electric Fuses and their Applications*, Maribor, 2011, pp. 219-224.

[20] M. Lindmayer, "3D simulation of fusing characteristics including the M-Effect," in *Proc. of the 6th Int. Conf. on Electric Fuses and their Applications,* Torino, 1999, pp. 13-20.

[21] E. Torres, E. Fernandez, A. J. Mazon, I. Zamora, and J. C. Perez, "Thermal analysis of medium voltage fuses using the finite element method," *IEEE Russia Power Tech*, pp. 1-5, 2005.

[22] A. A. Minea, "An experimental method to decrease heating time in a commercial furnace," *Experimental Heat Transf.*, vol. 23, pp. 175 – 184, 2010.

Adrian Pleşca was born in Iasi, Romania, on April 16, 1972. He graduated from the Gheorghe Asachi Technical University of Iaşi and he received the PhD degree in Electrical Engineering in 2001. His employment experience included the Gheorghe Asachi Technical University of Iasi, Power Engineering Department. His special fields of interest included electrical apparatus, special equipment for power semiconductor devices protection and 3D modelling and simulation of the electrical apparatus. Dr. Pleşca received Golden and Silver Medals at World Exhibition of Invention, Research and Industrial Innovation, Brussels, Belgium, EUREKA, 2001, 2004, Special Prize awarded by National Research Council of Thailand for Fundamental Research at The First International Invention's Day Convention, Bangkok, Thailand 2008, Gold Medal at 4th International Warsaw Invention Show 2010, Diploma and Genius Medal at 2nd International Invention Exhibition, Ljubljana, 2010 and Gold Prize at Seoul International Invention Fair, Korea 2011.